Experimental demonstration of the violation of the temporal Peres-Mermin inequality using contextual temporal correlations and noninvasive measurements

Dileep Singh,* Arvind,† and Kavita Dorai‡
Department of Physical Sciences, Indian Institute of Science Education & Research Mohali, Sector 81 SAS Nagar, Manauli PO 140306 Punjab, India

(Received 7 October 2021; accepted 15 February 2022; published 24 February 2022)

We present a generalized quantum scattering circuit which can be used to perform a noninvasive quantum measurement and implement it on NMR qubits. Such a measurement is a key requirement for testing temporal noncontextual inequalities. We use this circuit to experimentally demonstrate the violation of the Peres-Mermin inequality on a three-qubit NMR quantum information processor. Further, we experimentally construct a Bell-type inequality corresponding to the temporal Klyachko-Can-Binicioglu-Shumovsky (KCBS) inequality, and demonstrate that the maximum quantum correlation is achieved for four two-point correlation functions involved in this inequality. The experimental violation of all the inequalities matches well with the theoretically predicted values, within experimental errors.

DOI: 10.1103/PhysRevA.105.022216

I. INTRODUCTION

Intrinsic quantum correlations are used to distinguish between the quantum and classical realms and are an important resource for quantum information processing [1]. The Bell inequality was proposed in 1964, to provide bounds on classical correlations, and its violation implies inconsistency of locally realistic hidden variable models with quantum mechanics [2]. In a different direction to identify intrinsic quantumness, Kochen and Specker showed that quantum mechanics is contextual in the sense that it does not come under the purview of noncontextual hidden variable theories [3]. The concept of quantum contextuality was later extended to nonideal situations by including probabilistic hidden-variable models [4]. Hidden-variable theorems were derived to be applicable to real experimental situations with finite errors [5]. It was shown that the Hardy-type and GHZ-type proofs of the KS theorem involves a minimum of 18 vectors for any dimension, thereby verifying an old conjecture by Peres [6]. Recently, a noncontextual hidden variable model consistent with the kinematic predictions of quantum mechanics was proposed [7]; the set of quantum correlations that are possible for every Bell and Kochen-Specker type contextuality was derived using graph theory [8], and the role of contextuality in quantum key distribution (QKD) was explored [9]. Proofs of the Kochen-Specker theorem, developments in the area including experimental tests of quantum contextuality, and its connections with nonlocality, have been recently reviewed [10].

Klyachko-Can-Binicioglu-Shumovsky (KCBS) first proposed a state-dependent inequality to test noncontextuality of quantum correlations on a single qutrit (three-level indivisible quantum system) [11]. Since then there have been several state dependent and state independent proposals to test contextuality [9,12–14]. Experimental tests of quantum contextuality have been performed using photons [15], trapped ions [16,17], and nuclear spin qubits [18,19]. The lack of perfect compatibility due to errors in experiments that rely on sequential measurements to test noncontextual hidden variable models and methods to experimentally rule out certain hidden variable models which obey a generalized notion of noncontextuality are discussed in [20]. The original KS theorem was further extended to state independent inequalities and three experimentally testable inequalities were given which are valid for any noncontextual hidden variable theory and can be violated by any quantum state [21]. A twin KCBS inequality was also constructed to identify and characterize fully contextual quantum correlations [22]. An inequality, which used a set of nine dichotomic observables and involved compatible measurements on them, called the Peres-Mermin (PM) inequality, is considered the simplest proof of the KS theorem for a four-dimensional Hilbert space and relies on the construction of a Peres-Mermin square with elements of the square being combinations of Pauli measurements [23,24].

Bell-type inequalities are violated by quantum correlations that exist between spatially separated subsystems. An inequality to identify the intrinsic quantumness of temporal correlations, known as the Leggett-Garg (LG) inequality, assuming macroscopic realism and noninvasive measurements was constructed [25]. Such temporal quantum correlations can be revealed via noncommuting sequential measurements on the same system at different times. Later, generalized multiple-measurement LG inequalities were constructed and were interpreted using graph theory [26]. Temporal quantum correlations have also been posited to be a useful resource for quantum information processing protocols and recently a theoretical framework for unifying spatial and temporal correlations has been developed [27]. Extensions of LG-type

*dileepsingh@iisermohali.ac.in
†arvind@iisermohali.ac.in
‡kavita@iisermohali.ac.in

nonlocal realistic inequalities have been studied in the context of unsharp measurements [28,29]. A recent scheme demonstrated that temporal contextuality which is generated from sequential projective measurements, can be tested by violation of the KCBS inequality [30]. The structure of temporal correlations for a single-qubit system was characterized and experimental implementations on nitrogen-vacancy centers in diamond were explored [31]. The genuine multipartite nature of temporal correlations was confirmed by their simultaneous violation of pairwise temporal Clauser-Horne-Shimony-Holt (CHSH) inequalities [32]. The Tsirelson bound refers to the maximum degree up to which a Bell inequality can be violated [33] and is always less than the algebraic bound [34,35]. Tsirelson-type bounds provide maximal possible violation of Bell-type inequalities and such bounds have also been studied in the context of LG-type inequalities [36]. Achieving Tsirelson-type bounds in real experiments can be linked to the characterization of quantum devices via self-testing protocols. In this context, a self-testing protocol has been designed to certify Pauli measurements via the violation of an LG inequality [37]. Surprisingly for LG-type inequalities, it was found that the maximum degree to which the inequality can be violated is greater than the Tsirelson bound, and the violation increases with system size [38]. While the Bell theorem, the KS theorem and the LG inequality make different assumptions about physical reality, they all subscribe to the same underlying hypothesis, namely, that measurement outcomes in quantum mechanics are context independent. A framework was developed to convert a contextual scenario into equivalent temporal LG-type and spatial Bell-type inequalities [39].

Temporal noncontextuality inequalities typically require noninvasive measurements to capture temporal quantum correlations, a task not easy to perform experimentally. State-independent temporal noncontextuality inequalities were constructed and used to obtain lower bounds on the quantum dimension available to the measuring device [40]. It was shown that for measurements of dichotomous variables, the three-time LG inequalities cannot be violated beyond the Luders bound, which is numerically the same as the Tsirelson bound obeyed by Bell-type inequalities [41]. Violations of LG inequalities have been experimentally demonstrated using polarized photons [42,43], atomic ensembles [44], a hybrid optomechanical system [45], NMR systems [46–49], and superconducting qubits [50]. Recently, two- and three-time LG inequalities were experimentally implemented on an NMR system, using continuous in time velocity measurement and ideal negative measurement protocols [51]. Generalizations of LG tests have been proposed for Bose-Einstein condensates and atom interferometers [52].

In this work, we experimentally demonstrate the violation of a temporal contextuality PM inequality on an NMR quantum information processor, using three spin qubits. We generalize the quantum scattering circuit for two-point correlation functions given in Ref. [46] to measure n-point correlation functions, wherein an observable is measured sequentially in time. Performing n successive measurements allowed us to achieve a noninvasive measurement, without disturbing the subsequent evolution of the system. Unlike other measurement protocols, our circuit is able to measure the desired temporal correlations in a single experimental run and does not require additional CNOT and anti-CNOT gates. The violation of the temporal noncontextual inequality demonstrates the contextual nature of a particular quantum state during its time evolution. State-independent contextuality was tested via the violation of the temporal PM inequality, which was experimentally demonstrated by sequentially measuring the three-point correlation function and determining the expectation values of joint probabilities. We also experimentally explored the maximal violation of a Bell-type inequality corresponding to the temporal KCBS inequality, and demonstrate that the maximum possible quantum correlations are achieved for four two-point correlation functions. The measured experimental violation of the inequalities match well with the theoretically predicted bounds, within experimental errors.

This paper is organized as follows: The generalized quantum scattering circuit and its deployment in generating n-point time correlation functions is described in Sec. II. Section III A contains details of the NMR system and experimental parameters used for the implementation of the scattering circuit, while Sec. III B describes time correlation functions. Section III C describes the experimental demonstration of the violation of the temporal PM inequality, while Sec. III D contains details of the maximal experimental violation of a Bell-type inequality corresponding to the temporal KCBS inequality. Section III E contains a classical description of the experimental setup. Section IV offers a few concluding remarks about the scope and relevance of our work.

II. GENERALIZED QUANTUM SCATTERING CIRCUIT TO GENERATE TEMPORAL CORRELATIONS

Noninvasive measurements which do not disturb the subsequent evolution of a system are in general not possible in quantum mechanics. Several noncontextual inequalities such as the LG inequality or the temporal Bell-type inequalities require expectation values of the product of an observable at different times, to capture temporal quantum correlations. Ideally, one would imagine that noninvasive measurements would be required to compute such quantities. Experiments to carry out such noninvasive measurements are typically nontrivial to design and implement. We are able to use a generalized quantum scattering circuit to measure an n-time correlation function, which is equivalent to measuring the same observable at several different time points and taking the expectation value of the product, and with no interference produced by a measurement on subsequent measurements. It should be noted that if these individual measurements were to be carried out one by one, they would not be noninvasive in nature. While this equivalence is true according to a quantum mechanical description, it no longer holds if one assumes a nonclassical hidden variable description, and one would need to associate a measurement procedure with classical variables using the same experimental setup. We will take up a classical description of the experimental setup later on in this paper. Simulating the noninvasive measurement of the expectation value of the product of the same observable at different times via a single overall measurement is achieved via this generalized scattering circuit. We now describe our generalized quantum scattering circuit aimed at carrying out noninvasive

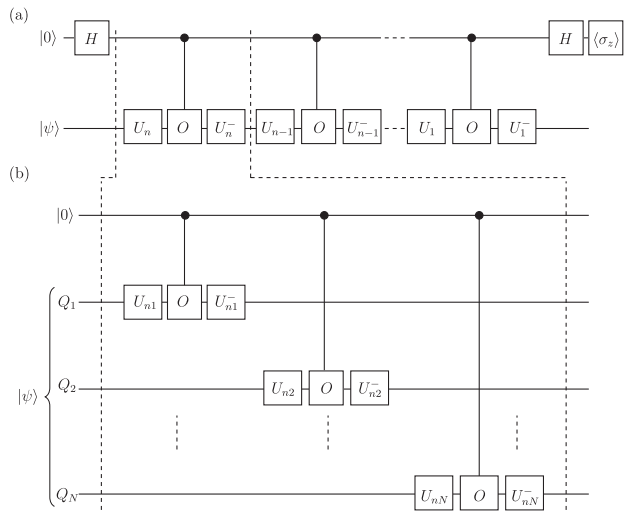

FIG. 1. (a) Generalized quantum scattering circuit to measure the n-point time correlation function $\langle[O_1(t_1)\otimes O_2(t_1)\cdots\otimes O_N(t_1)][O_1(t_2)\otimes O_2(t_2)\cdots\otimes O_N(t_2)]\ldots[O_1(t_n)\otimes O_2(t_n)\cdots\otimes O_N(t_n)]\rangle$, where each observable is a tensor product of N operators, $U_1^{\mp}=e^{\pm\frac{iHt_1}{\hbar}}$,... $U_{n-1}^{\mp}=e^{\pm\frac{iHt_{n-1}}{\hbar}}$, $U_n^{\mp}=e^{\pm\frac{iHt_n}{\hbar}}$. The "probe" (ancilla) qubit is initially in the state $|0\rangle$ and the system qubit is in the state $|\psi\rangle$. The correlation function is obtained by measuring the expectation value $\langle\sigma_z\rangle$ of the ancilla qubit. (b) Expanded schematic of the circuit between dotted lines in (a), showing the decomposition of the correlation function $\langle[O_1(t_n)\otimes O_2(t_n)\cdots\otimes O_N(t_n)]\rangle$, where $O_i(t_n)$ is measured on the ith qubit ($i=1...N$) and $|\psi\rangle$ refers to the initial state of all the system qubits and $U_{n1}^{\mp}=e^{\pm\frac{iHt_{n1}}{\hbar}}$, $U_{n2}^{\mp}=e^{\pm\frac{iHt_{n2}}{\hbar}}$..., $U_{nN}^{\mp}=e^{\pm\frac{iHt_{nN}}{\hbar}}$.

measurements which we will use to investigate the violation of temporal contextuality inequalities.

The standard quantum scattering circuit consists of a probe qubit (ancillary) and the system qubit(s). The generalized quantum scattering circuit which we have designed to compute n-point correlation functions involves performing n successive noninvasive measurements on an N-qubit quantum system, using only one ancilla qubit as the probe qubit. The circuit measures the n-point correlation function $\langle O(t_1)O(t_2)...O(t_n)\rangle$, wherein an observable is measured sequentially at time instants $t_1, t_2, ...t_n$.

Figure 1 depicts a schematic diagram of the generalized quantum scattering circuit to generate temporal correlations and demonstrate violation of temporal noncontextuality. The system is prepared in a known initial state, which interacts with the ancilla in such a way that a measurement over its state after the interaction, brings out the information about the system state. The "probe qubit" (ancillary qubit) is prepared in a known initial state and the "system qubit" is prepared in the state for which the observables are to be measured. The system is initially in the state $|\psi\rangle$, and is brought in contact with an ancilla qubit prepared in the state $|0\rangle$. This ancilla acts as a "probe particle" in the quantum scattering circuit. The circuit is implemented in three steps.

(1) A Hadamard gate is applied on the ancilla qubit.

(2) A "Controlled–U" operator is then applied (does nothing if the state of the ancilla is $|0\rangle$).

(3) A Hadamard gate is once again applied on the ancilla qubit and a measurement is performed on this qubit to detect its polarization (corresponding to measuring the expectation values of Pauli operators σ_z).

For noninvasive measurements, the input state of the system qubit has to be prepared in such a way that it is not affected by the application of the "Controlled-U" operator. This is achieved as follows.

The initial state is $|0\rangle\otimes|\psi\rangle$. After applying Hadamard on ancilla qubit, the state is transformed to $\frac{1}{\sqrt{2}}(|0\rangle+|1\rangle)\otimes|\psi\rangle$. Application of the Controlled-U operation changes the state to $\frac{1}{\sqrt{2}}(|0\rangle\otimes|\psi\rangle+|1\rangle\otimes U|\psi\rangle)$ with $U=e^{-iHt_1}Oe^{iHt_1}e^{-iHt_2}Oe^{iHt_2}\cdots$. Finally, the state after application of the second Hadamard gate on the ancilla qubit turns out to be

$$\frac{(|0\rangle+|1\rangle)\otimes|\psi\rangle+(|0\rangle-|1\rangle)\otimes U|\psi\rangle}{2}$$
$$=\frac{|0\rangle\otimes(I+U)|\psi\rangle+|1\rangle\otimes(I-U)|\psi\rangle}{2}.$$

Thus, if a measurement of the ancilla qubit in the computational basis yields the result $|0\rangle$, the state of the system qubit is $(I+U)|\psi\rangle$; however, if the measurement yields the result $|1\rangle$, the state of the system qubit is $(I-U)|\psi\rangle$. We note here that in this case, the operator U is a unitary because the observable O is a unitary (having only eigenvalues $+1$ or -1); however, this is in general not true for an arbitrary observable.

Consider the input state:

$$\rho_{\text{in}}=\rho_{\text{probe}}\otimes\rho_{\text{sys}}=|0\rangle\langle 0|\otimes|\psi\rangle\langle\psi|, \tag{1}$$

where the "probe qubit" is prepared in the $|0\rangle$ state and the "system qubit" is prepared in the state $|\psi\rangle$. After applying the unitary transformation shown in Fig. 1, the output is given by

$$\rho_{\text{out}}=|\psi_{\text{out}}\rangle\langle\psi_{\text{out}}|,\quad\text{with}$$
$$|\psi_{\text{out}}\rangle=|0\rangle\otimes(I+U)|\psi\rangle+|1\rangle\otimes(I-U)|\psi\rangle,\quad\text{and}$$
$$U=e^{\frac{iHt_1}{\hbar}}Oe^{-\frac{iHt_1}{\hbar}}e^{\frac{iHt_2}{\hbar}}Oe^{-\frac{iHt_2}{\hbar}}\cdots e^{\frac{iHt_n}{\hbar}}Oe^{-\frac{iHt_n}{\hbar}}. \tag{2}$$

The expectation of any operator A is given by $\sum_i p_i\lambda_i$, where p_i is the probability to get the eigenvalue λ_i. Hence

$$\langle\sigma_z\rangle=p_0-p_1, \tag{3}$$

where p_0 and p_1 are the probabilities to measure $|0\rangle$ with eigenvalue 1 and $|1\rangle$ eigenvalue -1, respectively. However, p_0 and p_1 are also equal to the probabilities of having the state of the system in $(I+U)|\psi\rangle$ with eigenvalue 1, and $(I-U)|\psi\rangle$ with eigenvalue -1, respectively.

Hence,

$$\begin{aligned}\langle\sigma_z\rangle&=\langle U\rangle=\text{Tr}(\rho_{sys}U)\\&=\langle\psi|e^{-iHt_1}Oe^{iHt_1}e^{-iHt_2}Oe^{iHt_2}\cdots|\psi\rangle\\&=\langle O(t_1).O(t_2)...\rangle,\end{aligned} \tag{4}$$

where the operators $O(t_1), O(t_2)$.... commute. Therefore, the real part of the expectation value of the z component of the spin angular momentum of the "probe" qubit turns out to be related to the expectation values of the desired observables of the original state.

The generalized quantum scattering circuit can be used to experimentally demonstrate those inequalities which involve temporal correlation functions, such as the temporal PM noncontextual inequality and the temporal KCBS inequality. While the ideal negative measurement (INM) protocol described in Ref. [51] is similar to our measurement scheme, in the INM protocol the ancilla is coupled to only one of the two measurement outcomes and the protocol hence requires two experimental runs: with a CNOT gate as well as with an anti-CNOT gate. Our circuit, on the other hand, requires only a single experimental run and does not require additional CNOT and anti-CNOT gates for its implementation.

III. VIOLATION OF TEMPORAL PM AND TEMPORAL BELL-TYPE INEQUALITIES

A. The NMR system

We used the molecule of ^{13}C-labeled diethyl fluoromalonate dissolved in acetone-D6 as a three-qubit system, with the ^{1}H, ^{19}F, and ^{13}C spin-1/2 nuclei being encoded as "qubit one," "qubit two," and "qubit three," respectively. The NMR Hamiltonian for a three-qubit system in the rotating frame is [53]

$$\mathcal{H} = -\sum_{i=1}^{3} \nu_i I_z^i + \sum_{i>j,i=1}^{3} J_{ij} I_z^i I_z^j, \tag{5}$$

where the indices $i, j = 1, 2$, or 3 label the qubit, ν_i is the chemical shift of the ith qubit in the rotating frame, J_{ij} is the scalar coupling interaction strength, and I_z^i is z component of the spin angular momentum operator of the i^{th} qubit. The system was initialized in a pseudopure state (PPS), i.e., $|000\rangle$, using the spatial averaging technique [54]. The fidelity of the experimentally prepared PPS state was computed to be 0.964 ± 0.004 using the Uhlmann-Jozsa fidelity measure [55,56]. Quantum state tomography was performed to experimentally reconstruct the density operator using a reduced tomography protocol [57]. The T_1 and T_2 relaxation times for all three qubits range between 3.7 s and 6.8 s and 1.0 s and 2.8 s, respectively. Nonlocal unitary operations were achieved by free evolution under the system Hamiltonian, of suitable duration under the desired scalar coupling with the help of embedded π refocusing pulses. The durations of the $\frac{\pi}{2}$ pulses for ^{1}H, ^{19}F, and ^{13}C nuclei were 9.55 μs at 18.14-W power level, 23.00 μs at a power level of 42.27 W, and 15.75 μs at a power level of 179.47 W, respectively.

B. Time-correlation functions

Consider performing a set of five dichotomic (i.e., the measurement outcomes are ± 1) measurements of variables X_j, $j = 1, ...5$ on a single system. Each measurement X_j is compatible with the preceding and succeeding measurements and the sums are modulo 5. Compatible measurements implies that the joint or sequential measurements of the variables X_j do not affect each other, which basically ensures that the measurements are noninvasive. We note here in passing that compatibility of the measurements must be verified classically as well, and one cannot assume the quantum mechanical properties (such as commutativity of operators) to justify noninvasive measurability from a classical perspective. The existence of a joint probability distribution for all the measurement outcomes can be tested by constructing the KCBS inequality [39]:

$$\sum_{j=0}^{4} \langle X_j X_{j+1} \rangle \geqslant -3, \tag{6}$$

where -3 is the minimum value for an NCHV model. Noncontextual in this sense implies that the NCHV theory assigns a value to an observable which is independent of other compatible observables being measured along with it. By definition each correlation function is given by [39]

$$\langle X_i X_j \rangle = \sum_{x_i, x_j = \pm 1} x_i x_j p(x_i, x_j). \tag{7}$$

A "pentagon LG" inequality was constructed wherein [26]

$$\sum_{1 \leqslant i < j \leqslant 5} \langle X_i X_j \rangle + 2 \geqslant 0. \tag{8}$$

This inequality has 10 two-time correlation functions which can be computed from one single experiment, wherein the measurements are performed in a manner such that the measurement of X_j does not affect the measurement outcome of X_i (noninvasive measurements). The two-time correlation function turns out to be [35]

$$\langle X_i X_j \rangle = \tfrac{1}{2} \mathrm{Tr}[\rho \{X_i, X_j\}] \tag{9}$$

for a density matrix ρ. The five measurable observables were chosen to be [40]

$$X_1 \equiv \sigma_z, X_2 \equiv \sigma_\theta, X_3 \equiv \sigma_z, X_4 \equiv \sigma_\theta, X_5 \equiv \sigma_z, \tag{10}$$

where σ_x, σ_z are the Pauli operators and $\sigma_\theta \equiv \cos\theta\, \sigma_z + \sin\theta\, \sigma_x$. For this set of chosen observables and with θ chosen such that $\cos\theta = -3/4$, the correlation function takes the value [26],

$$\sum_{1 \leqslant i < j \leqslant 5} \langle X_i X_j \rangle = -9/4, \tag{11}$$

which is the smallest possible value and violates the "pentagon" LG inequality given in Eq. (8).

C. Experimental violation of the temporal Peres-Mermin inequality

A temporal equivalent of the KCBS inequality can be constructed similarly to the "pentagon LG" inequality by considering a set of nine dichotomic variables, and three successive measurements at two sequential times from the set of time points $t = \{t_1, t_2, ..t_5\}$. The observable set chosen is the "PM square" of nine dichotomous and mutually compatible observables $A, B, C, a, b, c, \alpha, \beta, \gamma$ [40]:

$$\begin{aligned} &A = \sigma_z \otimes I, \quad B = I \otimes \sigma_z, \quad C = \sigma_z \otimes \sigma_z, \\ &a = I \otimes \sigma_x, \quad b = \sigma_x \otimes I, \quad c = \sigma_x \otimes \sigma_x, \\ &\alpha = \sigma_z \otimes \sigma_x, \quad \beta = \sigma_x \otimes \sigma_z, \quad \gamma = \sigma_y \otimes \sigma_y. \end{aligned} \tag{12}$$

Consider the combination of expectation values defined as follows:

$$\langle X_{\rm PM}\rangle = \langle ABC\rangle + \langle bca\rangle + \langle \gamma\alpha\beta\rangle + \langle A\alpha a\rangle + \langle bB\beta\rangle - \langle \gamma cC\rangle. \tag{13}$$

If we make noncontextual assignments of values we get the inequality,

$$\langle X_{\rm PM}\rangle \leqslant 4, \tag{14}$$

which is satisfied by all NCHV theories. This is the temporal PM inequality ($X_{\rm PM}$) [40]. It has been shown that for a four-dimensional quantum system and a particular set of observables, a value of $\langle X_{\rm PM}\rangle = 6$ is obtained for any quantum state, demonstrating state-independent contextuality [21].

We note here in passing that in this "PM square" set of measurements, each observable always occurs either in the first place or the second place or the third place in the sequential mean value. This inequality is violated whenever a joint probability distribution cannot be found which assigns predetermined outcomes to the measurements X_i at all times $t_1 \ldots t_5$, and this violation is termed contextual in time. The system evolves under the action of a time-independent Hamiltonian $H = \hbar\omega\sigma_{x,y}$, which can be implemented in NMR using suitable rf pulses applied on the qubits. After state preparation, the probe qubit interacts with the system qubit via suitable unitaries. The temporal correlation functions are obtained by measuring the real part of the expectation value of the z component of the spin angular momentum of the probe qubit.

Our experimental task is to measure the expectation values of joint probabilities which are measured sequentially. To violate the temporal PM inequality we need to measure the three observables sequentially for any two-qubit state. We experimentally violated the PM inequality by measuring the six correlation functions using the generalized quantum scattering circuit. Figure 2 shows the quantum scattering circuit, the operator decomposition, and the corresponding NMR pulse sequence, to calculate the correlation function $\langle A\alpha a\rangle$ which is one of the six correlation functions used in the PM temporal inequality. The PM temporal inequality is violated for any two-qubit state. The probe qubit is prepared in the known $|0\rangle$ state and the system qubit is prepared in the $|\phi\rangle = |00\rangle$ state. We apply the transformation given in Fig. 2(a), with suitable values of $O = \sigma_z$ and $\theta = \pi/2$. The correlation function $\langle A\alpha a\rangle$ for the $|\phi\rangle = |00\rangle$ state can be obtained by measuring the real part of the expected value of the z component of the spin for the probe qubit. The other correlation functions involved in the PM temporal inequality are measured in a similar fashion.

Since the temporal PM inequality is violated for any two-qubit state, we chose to prepare the probe qubit in a known $|0\rangle$ state and the system qubits were prepared in the $|\phi\rangle = |00\rangle$ state. The experimental tomograph of the state prepared in $\rho = |0\rangle\langle 0| \otimes |00\rangle\langle 00|$ is given in Fig. 3, achieved with a fidelity of 0.964 ± 0.004. We applied the unitary transformations given in Fig. 2 with values of $O = \sigma_z$ and $\theta = \pi/2$. The correlation function $\langle A\alpha a\rangle$ for the $|\phi\rangle = |00\rangle$ state can be obtained by measuring the real part of the expected value of the spin z component of the probe qubit. The other correlation functions involved in the temporal PM inequality are calculated in a similar fashion. The mean value of the correlation functions and their error bars were calculated by repeating the experiment three times and the theoretically expected and experimentally calculated values are given in Table I. The theoretically computed and experimentally measured values of the correlation functions agree well to within experimental errors. We experimentally violated the temporal PM inequality, obtaining $\langle X_{\rm PM}\rangle_{\rm Expt} = 4.667 \pm 0.013$, showing the contextual nature of the measured expectation values.

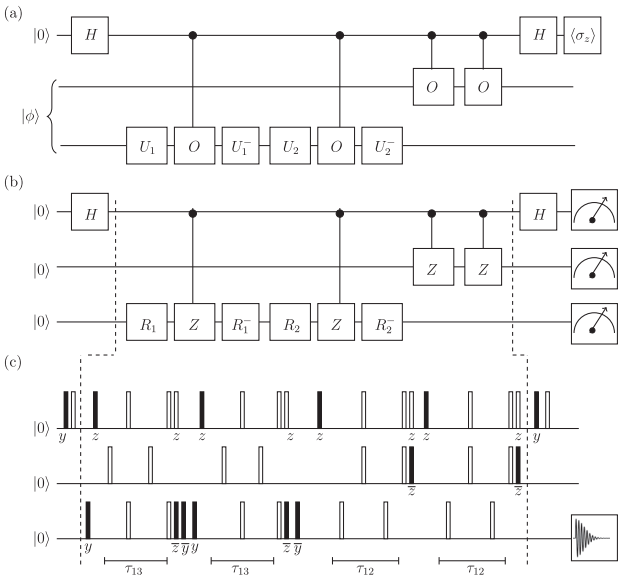

FIG. 2. (a) Quantum scattering circuit for measuring the correlation function $\langle A\alpha a\rangle$ involved in the PM inequality, where $O = \sigma_z$ and $U^{\pm}_{1,2} = e^{\mp i\sigma_y\theta/2}$ with $\theta = \pi/2$. (b) Decomposition of the quantum scattering circuit in terms of rotation operators where $R^{\pm}_{1,2}$ correspond to $(\frac{\pi}{2})_{\pm y}$, H are Hadamard gates, and Z are rotations about the z axis. (c) NMR pulse sequence corresponding to the quantum scattering circuit, where filled and unfilled rectangles correspond to $\pi/2$ and π pulses, respectively. The bar over a phase denotes negative phase. The time intervals τ_{12}, τ_{13} are set to $\frac{1}{2J_{\rm HF}}$ and $\frac{1}{2J_{\rm HC}}$, respectively.

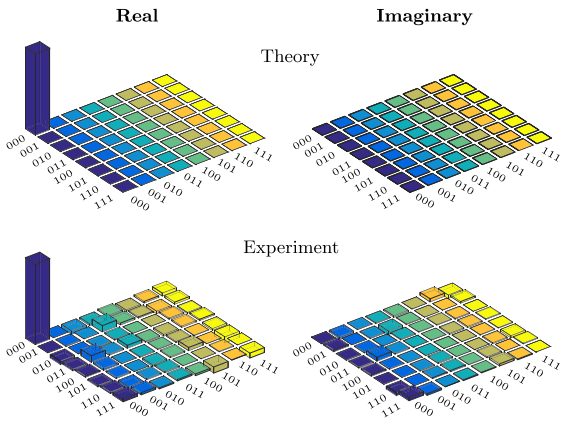

FIG. 3. Real (left) and imaginary (right) parts of the theoretical and experimental tomographs of the input $\rho = |0\rangle\langle 0| \otimes |00\rangle\langle 00|$ state in the eight-dimensional Hilbert space, prepared with an experimental state fidelity of 0.964 ± 0.004.

TABLE I. Theoretically computed and experimentally measured values of correlation functions corresponding to the PM inequality.

Observables	Theoretical	Experimental
$\langle ABC\rangle$	1	0.928 ± 0.017
$\langle bca\rangle$	1	0.706 ± 0.012
$\langle \gamma\alpha\beta\rangle$	1	0.817 ± 0.010
$\langle A\alpha a\rangle$	1	0.685 ± 0.008
$\langle bB\beta\rangle$	1	0.755 ± 0.011
$\langle \gamma cC\rangle$	-1	-0.784 ± 0.019

D. Maximal experimental violation of a Bell-type inequality corresponding to the temporal KCBS inequality

While it is clear that quantum correlations can violate spatial Bell-type and temporal LG-type inequalities, they do not go all the way to the values allowed by the no-signaling condition, and thus satisfy a bound called the Tsirelson's bound [33]. The reasons for the existence of such a bound which limits the algebraic values of the correlations between the measurement outcomes over and above the no-signaling condition, is still a matter of debate [34,35]. We construct here an experimental situation where the maximum possible quantum correlation is achieved for four two-point correlation functions involved in the temporal KCBS inequality when it is re-interpreted as a Bell-type inequality [39].

The temporal KCBS noncontextual inequality can be constructed by considering a dichotomic variable X_t with successive measurements performed at two sequential times drawn from the time instants $t = \{t_0, t_1, ..., t_4\}$. The two-point temporal correlations thus obtained lead to the corresponding temporal KCBS inequality [39]:

$$\sum_{i=0}^{4} \langle X_{t_i} X_{t_{i+1}} \rangle \geqslant -3. \tag{15}$$

The violation of this inequality can be termed as contextuality in time. The temporal KCBS inequality can be transformed into a Bell-type inequality which tests the existence of a joint probability distribution for measurements on dichotomic variables, performed on subsystems A and B. The Bell-type inequality is given by [39]

$$\langle A_0B_1\rangle + \langle A_1B_2\rangle + \langle A_2B_3\rangle + \langle A_3B_4\rangle + \langle A_4B_0\rangle \geqslant -3, \tag{16}$$

where A_i and B_j are measured on the subsystems with the additional constraint that

$$\langle A_iB_i\rangle = 1 \text{ for all } i, \tag{17}$$

which implies that the outcomes of pairs of measurements are the same. Violation of this inequality shows the nonexistence of joint probability distribution for this scenario.

We experimentally demonstrated the violation of the Bell-type inequality given in Eq. (16) using the quantum scattering circuit on the same three-qubit system. Figure 4(a) shows the quantum scattering circuit to calculate the correlation function $\langle A_rB_q\rangle$, involved in the Bell-type inequality on an eight-dimensional quantum system. For the violation of the Bell-type inequality, we used the ^{1}H as the probe qubit and ^{13}C and ^{19}F as the system qubits. We apply the transformations

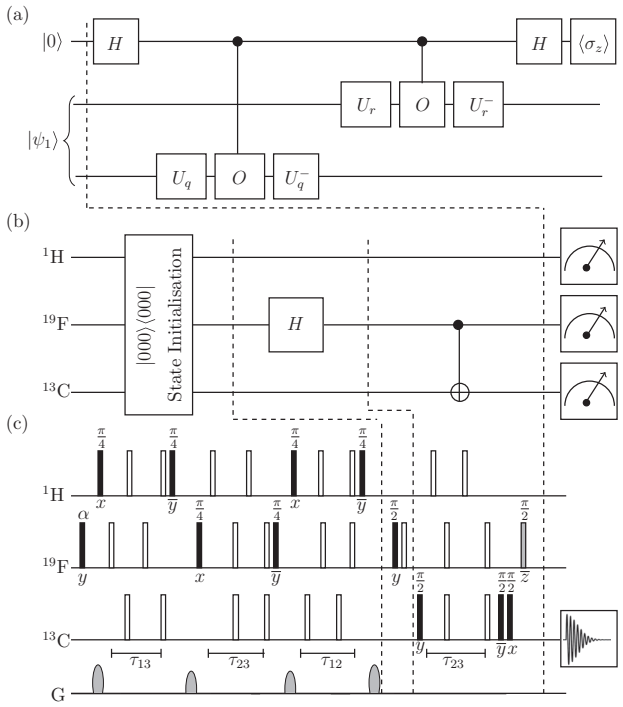

FIG. 4. (a) Quantum circuit to measure the correlation function $\langle A_rB_q\rangle$ involved in the Bell-type inequality, where $U_{r,q} = e^{\frac{-i2\pi r,q}{5}}$, $O = \sigma_z$ and $r, q = 0, 1, 2, 3, 4$. (b) Quantum circuit for state preparation. (c) Corresponding NMR pulse sequence for the quantum circuit. The sequence of pulses before the first dashed black line achieves initialization of the state into the pseudopure $|000\rangle$ state. The unfilled rectangles denote π pulses, and the flip angle and phases of the other pulses are written below each pulse. The bar over a phase indicates negative phase. The time intervals τ_{12}, τ_{13}, τ_{23} are set to $\frac{1}{2J_{\rm HF}}$, $\frac{1}{2J_{\rm HC}}$, $\frac{1}{2J_{\rm FC}}$, respectively.

given in Fig. 4(a) with suitable values of $O = \sigma_z$ and $q, r = 0, 1, 2, 3, 4$.

The optimal violation of the Bell-type inequality can be obtained for the state $\langle\psi_1| = \frac{1}{\sqrt{2}}(1, 0, 0, 1)$ with the probe qubit prepared in the state $|0\rangle$, and for the measurements $A_j = \sigma_j \otimes I$, $B_j = I \otimes \sigma_j$ where $j = 0, 1, 2, 3, 4$ and $\sigma_j = e^{i\frac{2\pi j}{5}\sigma_y}\sigma_z e^{-i\frac{2\pi j}{5}\sigma_y}$. The correlation functions $\langle A_rB_q\rangle$ for the state $\langle\psi_1| = \frac{1}{\sqrt{2}}(1, 0, 0, 1)$ can be obtained by measuring the real part of the expected value of the spin z component for the probe qubit. The corresponding quantum circuit for state preparation is shown in Fig. 4(b) and the NMR pulse sequence is shown in Fig. 4(c). The sequence of pulses before the first dashed black line achieves state initialization into the $|000\rangle$ state. After this we apply the Hadamard gate (on ^{13}C), followed by a CNOT$_{23}$ gate, and the resultant state corresponds to $\rho_1 = |0\rangle\langle 0| \otimes |\psi_1\rangle\langle\psi_1|$ with $\langle\psi_1| = \frac{1}{\sqrt{2}}(1, 0, 0, 1)$.

The tomograph of the state prepared in $\rho_1 = |0\rangle\langle 0| \otimes |\psi_1\rangle\langle\psi_1|$ with $\langle\psi_1| = \frac{1}{\sqrt{2}}(1, 0, 0, 1)$ is given in Fig. 5 with an experimental fidelity of 0.947 ± 0.009. The mean values of the correlation functions and their error bars were calculated by repeating the experiment three times and and calculated values are given in Table II. As seen from the values tabulated in Table II, the theoretically computed and

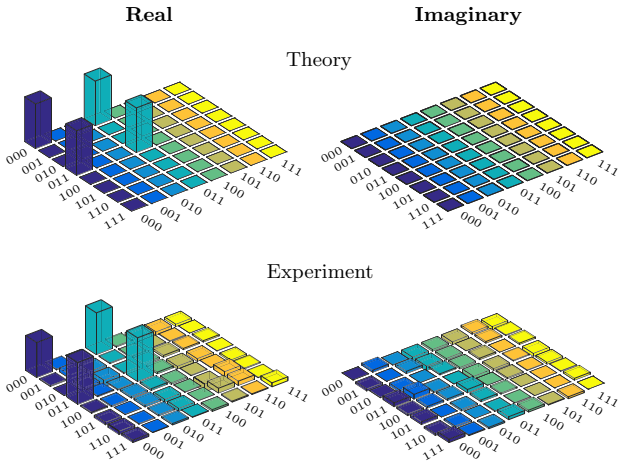

FIG. 5. Real (left) and imaginary (right) parts of the theoretically expected and the experimentally reconstructed tomographs of the $\langle\psi_1| = \frac{1}{\sqrt{2}}(1,0,0,1,0,0,0,0)$ state in the eight-dimensional quantum system, with an experimental state fidelity of 0.947 ± 0.009.

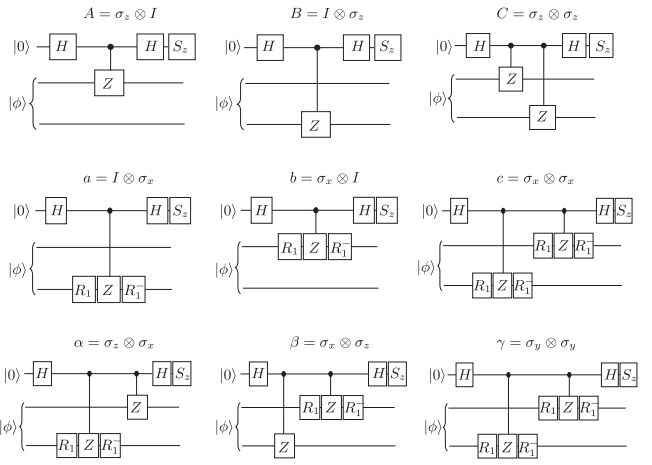

FIG. 6. Quantum scattering circuit for measuring the nine observables where $R_l^{\pm} = e^{\mp \frac{iH\sigma_y}{\hbar}}$ and $R_2^{\pm} = e^{\mp \frac{iH\sigma_x}{\hbar}}$; S_z denotes the expectation value of σ_z.

experimentally measured values of the correlation functions agree well to within experimental errors. We have experimentally violated the Bell-type inequality with the violation of -3.755 ± 0.008.

It should be noted that there are no spacelike separated measurements here. However, the inequality given in Eq. (16), with the constraint specified in Eq. (17), will be valid when the measurements on A and B are spacelike separated and when the no-signaling principle is relevant. Our limited goal here is to show the possibility of maximally violating the Bell-type inequality given in Eq. (16).

E. Classical description of the experimental setup

All experimental tests of nonclassical properties of quantum correlations whether quantum contextuality, Bell nonlocality, or nonclassical temporal correlations, ultimately seek to disprove a classical theory, either local hidden variable models, or noncontextual or macrorealist theories. Hence any experimental test of quantum correlations must subsume a classical description of the setup and one should be able to associate a measurement procedure to any classical variable using this setup. For instance, in order to measure the correlator $\langle AB\rangle$ one should in principle be able to measure A and B independently.

Throughout in our analysis we have considered expectation values of products of observables to show that a quantum description may violate bounds derived from classical ideas of assignment of outcomes to individual measurements. As mentioned above, it is important to be able to measure the observables one by one, where it is possible to imagine assigning outcomes from a classical description. To provide the possibility of a classical description of our experimental setup, we validate the following assumptions: (i) that each of the nine observables involved in the PM inequality can be measured individually and has the eigenvalue ± 1; and (ii) that the observables involved in the sequences of the PM inequality are mutually compatible.

TABLE II. Theoretically computed and experimentally measured values of quantum correlations corresponding to the Bell test.

Observables	Theoretical	Experimental
$\langle A_0B_1\rangle$	-0.809	-0.684 ± 0.014
$\langle A_1B_2\rangle$	-0.809	-0.754 ± 0.006
$\langle A_2B_3\rangle$	-0.809	-0.756 ± 0.011
$\langle A_3B_4\rangle$	-0.809	-0.746 ± 0.005
$\langle A_4B_0\rangle$	-0.809	-0.815 ± 0.004

TABLE III. Theoretically computed and experimentally measured values of each of the individual observables in their eigenstates.

Input State	Observables	Experimental (Theoretical)
$\|00\rangle$	$\sigma_z \otimes I$	$+0.945 \pm 0.026$ $(+1)$
$\|11\rangle$	$\sigma_z \otimes I$	-1.075 ± 0.027 (-1)
$\|00\rangle$	$I \otimes \sigma_z$	$+0.914 \pm 0.021$ $(+1)$
$\|11\rangle$	$I \otimes \sigma_z$	-0.901 ± 0.015 (-1)
$\|00\rangle$	$\sigma_z \otimes \sigma_z$	$+0.932 \pm 0.026$ $(+1)$
$\|10\rangle$	$\sigma_z \otimes \sigma_z$	-1.048 ± 0.029 (-1)
$\frac{\|00\rangle+\|01\rangle}{\sqrt{2}}$	$I \otimes \sigma_x$	$+0.969 \pm 0.025$ $(+1)$
$\frac{\|10\rangle-\|11\rangle}{\sqrt{2}}$	$I \otimes \sigma_x$	-0.993 ± 0.026 (-1)
$\frac{\|01\rangle+\|11\rangle}{\sqrt{2}}$	$\sigma_x \otimes I$	$+0.984 \pm 0.028$ $(+1)$
$\frac{\|01\rangle-\|11\rangle}{\sqrt{2}}$	$\sigma_x \otimes I$	-0.994 ± 0.029 (-1)
$\frac{\|00\rangle+\|11\rangle}{\sqrt{2}}$	$\sigma_x \otimes \sigma_x$	$+0.967 \pm 0.025$ $(+1)$
$\frac{\|00\rangle-\|11\rangle}{\sqrt{2}}$	$\sigma_x \otimes \sigma_x$	-0.97 ± 0.027 (-1)
$\frac{\|00\rangle+\|01\rangle}{\sqrt{2}}$	$\sigma_z \otimes \sigma_x$	$+1.067 \pm 0.023$ $(+1)$
$\frac{\|10\rangle+\|11\rangle}{\sqrt{2}}$	$\sigma_z \otimes \sigma_x$	-1.042 ± 0.021 (-1)
$\frac{\|00\rangle+\|10\rangle}{\sqrt{2}}$	$\sigma_x \otimes \sigma_z$	$+0.903 \pm 0.025$ $(+1)$
$\frac{\|01\rangle+\|11\rangle}{\sqrt{2}}$	$\sigma_x \otimes \sigma_z$	-0.975 ± 0.027 (-1)
$\frac{\|01\rangle+\|10\rangle}{\sqrt{2}}$	$\sigma_y \otimes \sigma_y$	$+1.001 \pm 0.012$ $(+1)$
$\frac{\|00\rangle+\|11\rangle}{\sqrt{2}}$	$\sigma_y \otimes \sigma_y$	-1.014 ± 0.026 (-1)

TABLE IV. Experimentally calculated expectation values of the possible combination of each observable of the six sequences to check the commutative relations.

Observables	Experimental	Observables	Experimental	Observables	Experimental
$\langle A.B.C\rangle$	0.928 ± 0.017	$\langle b.c.a\rangle$	0.706 ± 0.012	$\langle \gamma.\alpha.\beta\rangle$	0.817 ± 0.010
$\langle A.C.B\rangle$	0.935 ± 0.012	$\langle b.a.c\rangle$	0.723 ± 0.010	$\langle \gamma.\beta.\alpha\rangle$	0.839 ± 0.012
$\langle B.A.C\rangle$	0.919 ± 0.009	$\langle a.b.c\rangle$	0.725 ± 0.019	$\langle \alpha.\beta.\gamma\rangle$	0.829 ± 0.010
$\langle B.C.A\rangle$	0.935 ± 0.008	$\langle a.c.b\rangle$	0.707 ± 0.015	$\langle \alpha.\gamma.\beta\rangle$	0.799 ± 0.018
$\langle C.A.B\rangle$	0.929 ± 0.012	$\langle c.a.b\rangle$	0.733 ± 0.018	$\langle \beta.\alpha.\gamma\rangle$	0.824 ± 0.014
$\langle C.B.A\rangle$	0.908 ± 0.010	$\langle c.b.a\rangle$	0.719 ± 0.017	$\langle \beta.\gamma.\alpha\rangle$	0.796 ± 0.016
$\langle A.\alpha.a\rangle$	0.685 ± 0.008	$\langle b.B.\beta\rangle$	0.755 ± 0.011	$\langle \gamma.c.C\rangle$	-0.784 ± 0.019
$\langle A.a.\alpha\rangle$	0.672 ± 0.017	$\langle b.\beta.B\rangle$	0.726 ± 0.019	$\langle \gamma.C.c\rangle$	-0.813 ± 0.010
$\langle \alpha.A.a\rangle$	0.671 ± 0.018	$\langle B.b.\beta\rangle$	0.776 ± 0.017	$\langle C.\gamma.c\rangle$	-0.760 ± 0.020
$\langle \alpha.a.A\rangle$	0.644 ± 0.020	$\langle B.\beta.b\rangle$	0.779 ± 0.009	$\langle C.c.\gamma\rangle$	-0.811 ± 0.012
$\langle a.A.\alpha\rangle$	0.714 ± 0.017	$\langle \beta.B.b\rangle$	0.776 ± 0.015	$\langle c.C.\gamma\rangle$	-0.771 ± 0.019
$\langle a.\alpha.A\rangle$	0.639 ± 0.019	$\langle \beta.b.B\rangle$	0.746 ± 0.019	$\langle c.\gamma.C\rangle$	-0.789 ± 0.013

We first check that each observable in the PM inequality has the eigenvalue ± 1. To do so, we measure the expectation values of the nine individual observables using the quantum scattering circuit given in Fig. 6. The input states are prepared in the eigenstates of each of the nine observables involved in the PM inequality. Table III contains a comparison of the experimentally observable expectation values of each observable with its theoretically expected value of ± 1.

We then proceed to check the second assumption that the measurements in the six sequences involved in the PM inequality are commutative, i.e., each of the observables is context independent. We do this by switching the measurement sequence in the scattering circuit. Table IV contains the experimentally calculated expectation values of all possible combinations of each observable in the six sequences involved in the PM inequality.

IV. CONCLUDING REMARKS

We designed and experimentally implemented a generalized quantum scattering circuit to measure an n-point correlation function on an NMR quantum information processor, with an observable being measured sequentially at these n time instants. We experimentally demonstrated the violation of a temporal noncontextuality PM inequality using three NMR qubits, which involved performing sequential noninvasive measurements. The generalized quantum scattering circuit we have constructed is independent of the quantum hardware used for its implementation and can be applied to systems other than NMR qubits. Our work asserts that NMR quantum processors can serve as optimal test beds for testing such inequalities.

ACKNOWLEDGMENTS

All the experiments were performed on a Bruker Avance-III 600 MHz FT-NMR spectrometer at the NMR Research Facility of IISER Mohali. Arvind acknowledges financial support from DST/ICPS/QuST/2019/Q68. K.D. acknowledges financial support from DST/ICPS/QuST/2019/Q74.

[1] M. A. Nielsen and I. L. Chuang, *Quantum Computation and Quantum Information* (Cambridge University Press, Cambridge, 2010).
[2] J. S. Bell, Physics **1**, 195 (1964).
[3] S. Kochen and E. P. Specker, J. Math. Mech. **17**, 59 (1967).
[4] J.-A. Larsson, Europhys. Lett. **58**, 799 (2002).
[5] C. Simon, C. Brukner, and A. Zeilinger, Phys. Rev. Lett. **86**, 4427 (2001).
[6] Z.-P. Xu, J.-L. Chen, and O. Gühne, Phys. Rev. Lett. **124**, 230401 (2020).
[7] A. S. Arora, K. Bharti, and Arvind, Phys. Lett. A **383**, 833 (2019).
[8] A. Cabello, Phys. Rev. A **100**, 032120 (2019).
[9] J. Singh, K. Bharti, and Arvind, Phys. Rev. A **95**, 062333 (2017).
[10] C. Budroni, A. Cabello, O. Guhne, M. Kleinmann, and J.-A. Larsson, arXiv:2102.13036.
[11] A. A. Klyachko, M. A. Can, S. Binicioğlu, and A. S. Shumovsky, Phys. Rev. Lett. **101**, 020403 (2008).
[12] P. Kurzynski and D. Kaszlikowski, Phys. Rev. A **86**, 042125 (2012).
[13] A. Cabello, M. Kleinmann, and C. Budroni, Phys. Rev. Lett. **114**, 250402 (2015).
[14] A. Sohbi, I. Zaquine, E. Diamanti, and D. Markham, Phys. Rev. A **94**, 032114 (2016).
[15] E. Nagali, V. D'Ambrosio, F. Sciarrino, and A. Cabello, Phys. Rev. Lett. **108**, 090501 (2012).
[16] G. Kirchmair, F. Zahringer, R. Gerritsma, M. Kleinmann, O. Guhne, A. Cabello, R. Blatt, and C. F. Roos, Nature (London) **460**, 494 (2009).
[17] F. M. Leupold, M. Malinowski, C. Zhang, V. Negnevitsky, J. Alonso, J. P. Home, and A. Cabello, Phys. Rev. Lett. **120**, 180401 (2018).
[18] S. Dogra, K. Dorai, and Arvind, Phys. Lett. A **380**, 1941 (2016).

[19] D. Singh, J. Singh, K. Dorai, and Arvind, Phys. Rev. A **100**, 022109 (2019).
[20] O. Gühne, M. Kleinmann, A. Cabello, J.-A. Larsson, G. Kirchmair, F. Zähringer, R. Gerritsma, and C. F. Roos, Phys. Rev. A **81**, 022121 (2010).
[21] A. Cabello, Phys. Rev. Lett. **101**, 210401 (2008).
[22] A. Cabello, Phys. Rev. A **87**, 010104(R) (2013).
[23] A. Peres, Phys. Lett. A **151**, 107 (1990).
[24] N. D. Mermin, Phys. Rev. Lett. **65**, 3373 (1990).
[25] A. J. Leggett and A. Garg, Phys. Rev. Lett. **54**, 857 (1985).
[26] D. Avis, P. Hayden, and M. M. Wilde, Phys. Rev. A **82**, 030102(R) (2010).
[27] F. Costa, M. Ringbauer, M. E. Goggin, A. G. White, and A. Fedrizzi, Phys. Rev. A **98**, 012328 (2018).
[28] A. Rai, D. Home, and A. S. Majumdar, Phys. Rev. A **84**, 052115 (2011).
[29] D. Saha, S. Mal, P. K. Panigrahi, and D. Home, Phys. Rev. A **91**, 032117 (2015).
[30] G.-Z. Pan, G. Zhang, and Q.-H. Sun, Int. J. Theor. Phys. **32**, 2550 (2019).
[31] J. Hoffmann, C. Spee, O. Gühne, and C. Budroni, New J. Phys. **20**, 102001 (2018).
[32] M. Ringbauer, F. Costa, M. E. Goggin, A. G. White, and A. Fedrizzi, npj Quantum Inf. **4**, 37 (2018).
[33] B. S. Tsirel'son, J. Sov. Math. **36**, 557 (1987).
[34] M. Navascues, S. Pironio, and A. Acin, Phys. Rev. Lett. **98**, 010401 (2007).
[35] T. Fritz, New J. Phys. **12**, 083055 (2010).
[36] S. Mal and A. Majumdar, Phys. Lett. A **380**, 2265 (2016).
[37] A. G. Maity, S. Mal, C. Jebarathinam, and A. S. Majumdar, Phys. Rev. A **103**, 062604 (2021).
[38] C. Budroni and C. Emary, Phys. Rev. Lett. **113**, 050401 (2014).
[39] M. Markiewicz, P. Kurzynski, J. Thompson, S.-Y. Lee, A. Soeda, T. Paterek, and D. Kaszlikowski, Phys. Rev. A **89**, 042109 (2014).
[40] O. Guhne, C. Budroni, A. Cabello, M. Kleinmann, and J.-A. Larsson, Phys. Rev. A **89**, 062107 (2014).
[41] J. J. Halliwell and C. Mawby, Phys. Rev. A **102**, 012209 (2020).
[42] M. E. Goggin, M. P. Almeida, M. Barbieri, B. P. Lanyon, J. L. O'Brien, A. G. White, and G. J. Pryde, Proc. Natl. Acad. Sci. USA **108**, 1256 (2011).
[43] J. Dressel, C. J. Broadbent, J. C. Howell, and A. N. Jordan, Phys. Rev. Lett. **106**, 040402 (2011).
[44] C. Budroni, G. Vitagliano, G. Colangelo, R. J. Sewell, O. Gühne, G. Tóth, and M. W. Mitchell, Phys. Rev. Lett. **115**, 200403 (2015).
[45] M. Marchese, H. McAleese, A. Bassi, and M. Paternostro, J. Phys. B: At. Mol. Opt. Phys. **53**, 075401 (2020).
[46] A. M. Souza, I. S. Oliveira, and R. S. Sarthour, New J. Phys. **13**, 053023 (2011).
[47] V. Athalye, S. S. Roy, and T. S. Mahesh, Phys. Rev. Lett. **107**, 130402 (2011).
[48] H. Katiyar, A. Shukla, K. R. K. Rao, and T. S. Mahesh, Phys. Rev. A **87**, 052102 (2013).
[49] H. Katiyar, A. Brodutch, D. Lu, and R. Laflamme, New J. Phys. **19**, 023033 (2017).
[50] E. Huffman and A. Mizel, Phys. Rev. A **95**, 032131 (2017).
[51] S.-S. Majidy, H. Katiyar, G. Anikeeva, J. Halliwell, and R. Laflamme, Phys. Rev. A **100**, 042325 (2019).
[52] L. Rosales-Zárate, B. Opanchuk, Q. Y. He, and M. D. Reid, Phys. Rev. A **97**, 042114 (2018).
[53] I. S. Oliveira, T. J. Bonagamba, R. S. Sarthour, J. C. C. Freitas, and E. R. deAzevedo, *NMR Quantum Information Processing* (Elsevier, Oxford, 2007).
[54] D. G. Cory, M. D. Price, and T. F. Havel, Physica D **120**, 82 (1998).
[55] R. Jozsa, J. Mod. Opt. **41**, 2315 (1994).
[56] A. Uhlmann, Rep. Math. Phys. **9**, 273 (1976).
[57] G. M. Leskowitz and L. J. Mueller, Phys. Rev. A **69**, 052302 (2004).